

This is the accepted manuscript made available via CHORUS. The article has been published as:

# Numerical Simulation of Finite-Temperature Field Theory for Interacting Bosons

Kris T. Delaney, Henri Orland, and Glenn H. Fredrickson

Phys. Rev. Lett. **124**, 070601 — Published 19 February 2020

DOI: [10.1103/PhysRevLett.124.070601](https://doi.org/10.1103/PhysRevLett.124.070601)

# Numerical Simulation of Finite-Temperature Field Theory for Interacting Bosons

Kris T. Delaney,<sup>1</sup> Henri Orland,<sup>2</sup> and Glenn H. Fredrickson<sup>1,3</sup>

<sup>1</sup>*Materials Research Laboratory, University of California, Santa Barbara, CA 93106-5121, USA*

<sup>2</sup>*Institut de Physique Théorique, CE-Saclay, CEA, F-91191 Gif-sur-Yvette Cedex, France*

<sup>3</sup>*Departments of Materials and Chemical Engineering,  
University of California, Santa Barbara, CA 93106, USA*

(Dated: January 15, 2020)

We report a stable and efficient complex Langevin sampling scheme for performing approximation-free numerical simulations directly on the path-integral coherent-states field theory for an assembly of interacting bosons. We apply the method to generate the  $\lambda$  line of critical phase transitions associated with Bose-Einstein condensation (BEC) in a model  $\phi^4$  scalar field theory. The new approach enjoys near-linear scaling in the resolved  $(d+1)$  spatial / imaginary-time dimensions and should be particularly efficient for the study of dense systems at low temperature.

PACS numbers: 67.10.Fj, 67.85.Hj, 67.25.dj

*Introduction:* Low-temperature assemblies of identical bosons exhibit fascinating quantum phenomena, including superfluidity[1, 2] and Bose-Einstein condensation[3–5]. The development of magneto-optical trapping[6] and evaporative cooling techniques[7] have allowed ultra-cold gases to be confined to different kinds of atom traps at extreme low temperatures in the nK range. This has further enabled a significant effort in creating optical lattices to study fundamental many-body phenomena, including the quantum critical point at the crossover from superfluid to Mott insulator[8–11].

Computer simulations have an important role to play in low-temperature physics in guiding experiment design and interpreting outcomes. The dominant simulation approach for finite-temperature, equilibrium quantum statistical mechanics of identical bosons in continuous space is provided by path-integral Monte Carlo[12] (PIMC), which uses the position representation of the thermal density matrix to sample particle degrees of freedom at a discrete set of imaginary times. Although PIMC has been successfully applied to a wide range of finite-temperature quantum many-body problems[12–17], and advanced PIMC sampling algorithms have been developed (e.g., the continuous-space worm algorithm[18]), one drawback of PIMC remains the requirement to track the coordinates of every particle at numerous imaginary-time intervals, and the need to explicitly sample particle exchange permutations to correctly symmetrize the thermal density matrix. This renders the method considerably more demanding at low temperature and/or high particle density.

Our work begins with the second-quantized description of a many-boson partition function, with particle exchange statistics embedded in the commutation relations of the raising and lowering operators of the many-body Hilbert space. By transforming the path integral to the basis of bosonic coherent-states[19], a field-theory representation emerges that is implicitly symmetric in the boson coordinates, removing the requirement to explicitly

sample particle exchange permutations. However, the resulting field theory contains a sign problem: the statistical weight, which contains the exponential of an action functional that is extensive with system size, has a wildly oscillating phase with variations in the coherent-states fields, resulting in exponentially vanishing normalization factors that render sampling intractable. Since the action is analytic in the field variables for such bosonic theories, complex Langevin (CL) sampling proves to be a general technique to bypass this sign problem[20, 21] by adaptively sampling along near-stationary-phase trajectories in an analytically continued field theory. Although there is no general guarantee of convergence, it has been proven[22] that complex Langevin simulations that converge to time-independent ensemble averages are free of any bias. Despite the promise of implicit symmetrization without a sign problem, the adoption of the CL approach has been hindered by the relative lack of stable and efficient algorithms, apart from limited application to model systems in high-energy physics[23–25]. In this Letter, we introduce a new general complex-Langevin algorithm for sampling of the coherent-states field theory of a low-temperature assembly of bosons and demonstrate its application by mapping the  $\lambda$  line of critical phase transitions in a  $\phi^4$  scalar field theory.

*Methods:* The path-integral representation of the grand partition function,  $\Xi$ , in a basis of spinless-boson coherent-state fields,  $\varphi_n(\mathbf{r})$ , where  $n \in [0, N_\tau]$  is a discrete imaginary-time index, can be written as

$$\Xi(\mu, V, T) = \prod_{n=0}^{N_\tau-1} \int_{\varphi_{N_\tau} = \varphi_0} \mathcal{D}(\varphi_n^*, \varphi_n) e^{-S[\{\varphi_n^*\}, \{\varphi_n\}]} \quad (1)$$

The grand-partition function involves a functional integral over real and imaginary parts of the complex-valued fields,  $\varphi_n(\mathbf{r})$ , which are taken with periodic boundary conditions in imaginary time,  $\varphi_{N_\tau}(\mathbf{r}) = \varphi_0(\mathbf{r})$ . The complex-conjugate field is denoted  $\varphi_n^*(\mathbf{r})$ . The action functional,  $S$ , contains the link between imaginary time

slices, one-body operators for kinetic energy, external po-

tential  $U_{\text{ext}}$  and chemical potential  $\mu$ , and a two-body term for pair interactions between bosons,  $v$ :

$$S[\{\varphi_n^*\}, \{\varphi_n\}] = \sum_{n=0}^{N_\tau-1} \int d\mathbf{r} \varphi_n^*(\mathbf{r}) \left[ \varphi_n(\mathbf{r}) - \varphi_{n-1}(\mathbf{r}) + \varepsilon \left( -\frac{\hbar^2}{2m} \nabla^2 + U_{\text{ext}}(\mathbf{r}) - \mu \right) \varphi_{n-1}(\mathbf{r}) \right] + \frac{\varepsilon}{2} \sum_{n=0}^{N_\tau-1} \int d\mathbf{r} \int d\mathbf{r}' \varphi_n^*(\mathbf{r}) \varphi_{n-1}(\mathbf{r}) v(|\mathbf{r} - \mathbf{r}'|) \varphi_n^*(\mathbf{r}') \varphi_{n-1}(\mathbf{r}'), \quad (2)$$

where  $\varepsilon = \beta/N_\tau$  and  $\beta = 1/k_B T$ . In this work, we employ periodic boundary conditions in spatial coordinates throughout.

Thermodynamic observables, e.g.,  $O$ , can be written as ensemble averages over field configurations  $O = \langle \tilde{O}[\varphi, \varphi^*] \rangle$ , of a coherent-states field operator  $\tilde{O}[\varphi, \varphi^*]$ , where the average is taken with a complex-valued statistical weight  $\exp(-S)$ . Example operators include the particle number,  $\tilde{N}[\varphi, \varphi^*] = \frac{1}{N_\tau} \sum_{n=0}^{N_\tau-1} \int d\mathbf{r} \varphi_n^*(\mathbf{r}) \varphi_{n-1}(\mathbf{r})$ , the density matrix,  $\tilde{\rho}(\mathbf{r}, \mathbf{r}'; [\varphi, \varphi^*]) = \frac{1}{N_\tau} \sum_{n=0}^{N_\tau-1} \varphi_n^*(\mathbf{r}) \varphi_{n-1}(\mathbf{r}')$ , and the imaginary-time Green function,  $\tilde{G}_n(\mathbf{r}, \mathbf{r}'; [\varphi, \varphi^*]) = \varphi_0^*(\mathbf{r}) \varphi_{n-1}(\mathbf{r}')$ . Note that while thermodynamic observables are necessarily real-valued, instantaneous operator values will be complex prior to ensemble averaging.

Since the action functional in Eqn. 2 is complex valued and extensive, the coherent-states field theory suffers from a sign problem that renders traditional sampling methods practically inapplicable. Complex Langevin[20, 21] (CL) dynamics is a fictitious stochastic dynamics that bypasses the sign problem in sampling the complex-valued statistical weight of the field theory. Within this approach, both the real and imaginary parts of the field are treated as independent and are individually analytically continued to the full complex plane; a stochastic process then samples field configurations, evolving to near-stationary-phase trajectories, and operator averages are computed over the fictitious time. Following our algorithmic development for a similar form of classical polymer field theories[26], we have found that an off-diagonal relaxation scheme that decouples  $\varphi$  and  $\varphi^*$  to linear order allows for stable time stepping of the complex Langevin equations. In this scheme, the CL equations of motion become

$$\begin{aligned} \partial_t \varphi_n(\mathbf{r}, t) &= -\frac{\delta S[\{\varphi_n^*\}, \{\varphi_n\}]}{\delta \varphi_n^*(\mathbf{r}, t)} + \gamma_n(\mathbf{r}, t) \\ \partial_t \varphi_n^*(\mathbf{r}, t) &= -\frac{\delta S[\{\varphi_n^*\}, \{\varphi_n\}]}{\delta \varphi_n(\mathbf{r}, t)} + \gamma_n^*(\mathbf{r}, t) \end{aligned} \quad (3)$$

where  $\varphi_n$  and  $\varphi_n^*$  are understood to be independent, complex-valued fields, and  $t$  is the fictitious (Langevin) time. These equations include relaxation

terms from cross functional derivatives of the action and driving noise. In order to satisfy the fluctuation-dissipation theorem for this dynamics selection, the Langevin noise terms must be appropriately correlated:  $\gamma_n(\mathbf{r}, t) = \frac{1}{\sqrt{2}} \left( \eta_n^{(1)}(\mathbf{r}, t) + i\eta_n^{(2)}(\mathbf{r}, t) \right)$ , where the  $\eta$  are real-valued Gaussian random variables with variance  $\langle \eta_n^{(i)}(\mathbf{r}, t) \eta_m^{(j)}(\mathbf{r}', t') \rangle = 2\delta_{ij} \delta_{nm} \delta(\mathbf{r} - \mathbf{r}') \delta(t - t')$ , and  $\gamma_n^*(\mathbf{r}, t)$  is the complex conjugate of  $\gamma_n(\mathbf{r}, t)$ . The scheme presented here is equivalent to one obtained[24] by writing conventional CL equations of motion[20, 21] for real-valued fields  $u(\mathbf{r})$ ,  $v(\mathbf{r})$  that are subsequently complexified, with  $\varphi(\mathbf{r}) \propto u(\mathbf{r}) + iv(\mathbf{r})$  and  $\varphi^*(\mathbf{r}) \propto u(\mathbf{r}) - iv(\mathbf{r})$ .

We develop a pseudospectral method for sampling Eqn. 3. Functions of spatial coordinates are transformed according to the Fourier convention  $g_{\mathbf{k}} = V^{-1} \int d\mathbf{r} f(\mathbf{r}) \exp(-i\mathbf{k} \cdot \mathbf{r})$ , where  $\mathbf{k}$  are translation vectors of the reciprocal cell:  $2\pi L^{-1}(l, m, n)$  for  $l, m, n \in \mathbb{Z}$ , assuming a cubic simulation cell of side  $L$ . Similarly, functions of the discrete imaginary-time variable are transformed to imaginary Matsubara frequencies using the Fourier convention  $g_m = N_\tau^{-1} \sum_{n=0}^{N_\tau-1} f_n \exp(-in\varepsilon\omega_j)$  with  $\omega_j = 2\pi j/\beta$  for  $j \in \mathbb{Z}$ . The resulting continuous-time CL equations of motion, which are approximation free in the  $N_\tau \rightarrow \infty$  limit, are:

$$\partial_t \psi_{\mathbf{k}j}(t) = -A_{\mathbf{k}j} \psi_{\mathbf{k}j}(t) + \mathcal{F}_2(\gamma_n(\mathbf{r}, t)) \quad (4)$$

$$- \mathcal{F}_2[\varepsilon w_n(\mathbf{r}, t; [\{\varphi_n^*\}, \{\varphi_n\}]) \varphi_{n-1}(\mathbf{r}, t)]$$

$$\partial_t \psi_{\mathbf{k}j}^*(t) = -A_{\mathbf{k}j}^* \psi_{\mathbf{k}j}^*(t) + \mathcal{F}_2(\gamma_n^*(\mathbf{r}, t)) \quad (5)$$

$$- \mathcal{F}_2[\varepsilon w_{n+1}(\mathbf{r}, t; [\{\varphi_n^*\}, \{\varphi_n\}]) \varphi_{n+1}^*(\mathbf{r}, t)]$$

where  $A_{\mathbf{k}j} = 1 - (1 - \varepsilon \hbar^2 k^2 / 2m + \varepsilon \mu) e^{-2\pi i j / N_\tau}$ ,  $w_n(\mathbf{r}) = U_{\text{ext}}(\mathbf{r}) + \int d\mathbf{r}' v(|\mathbf{r} - \mathbf{r}'|) \varphi_n^*(\mathbf{r}') \varphi_{n-1}(\mathbf{r}')$ ,  $\mathcal{F}_2(f_n(\mathbf{r}))$  denotes the Fourier transform over both space and imaginary time, and  $\psi_{\mathbf{k}j} = \mathcal{F}_2(\varphi_n(\mathbf{r}))$ ,  $\psi_{\mathbf{k}j}^* = \mathcal{F}_2(\varphi_n^*(\mathbf{r}))$ . Note that while  $\psi_{\mathbf{k},j}^*$  and  $\psi_{\mathbf{k},j}$  denote two independent complex variables in the complex Langevin sampling scheme, the linear coefficient  $A_{\mathbf{k},j}^*$  is precisely the complex conjugate of  $A_{\mathbf{k},j}$ . Importantly, Eqns. 4 and 5 provide insight into expected numerical time-integration stability for finite  $N_\tau$ . Analytic linear stability demands that  $\Re(A_{\mathbf{k}j}) > 0$ , which is also the condition for the ideal-gas quadratic action to be positive definite, required for the Gaussian-integral identities used to

construct the partition function. It is thus easily demonstrated that  $0 < \varepsilon(\hbar^2 k^2/2m - \mu) < 2$  is required for linear stability, so that  $N_\tau > \beta(\hbar^2 k_{\max}^2/2m - \mu)/2$  defines a minimal number of imaginary-time samples for the wave vector cutoff,  $k_{\max}$ , in the computational lattice.

To numerically propagate the pseudospectral equations of motion in time by discrete steps  $\Delta t$ , we take the linear coefficient  $A_{\mathbf{k}j}$  as an integrating factor over the  $\Delta t$  interval resulting in an exponential-time-differencing

$$\psi_{\mathbf{k}j}^{(l+1)} \approx e^{-A_{\mathbf{k}j}\Delta t} \psi_{\mathbf{k}j}^{(l)} - \left[ \frac{1 - e^{-A_{\mathbf{k}j}\Delta t}}{A_{\mathbf{k}j}} \right] \mathcal{F}_2 \left[ \varepsilon w_n^{(l)}(\mathbf{r}) \varphi_{n-1}^{(l)}(\mathbf{r}) \right] + R_{\mathbf{k}j}^l \quad (6)$$

$$(\psi_{\mathbf{k}j}^*)^{(l+1)} \approx e^{-A_{\mathbf{k}j}^*\Delta t} (\psi_{\mathbf{k}j}^*)^{(l)} - \left[ \frac{1 - e^{-A_{\mathbf{k}j}^*\Delta t}}{A_{\mathbf{k}j}^*} \right] \mathcal{F}_2 \left[ \varepsilon w_{n+1}^{(l)}(\mathbf{r}) (\varphi_{n+1}^*(\mathbf{r}))^{(l)} \right] + (R_{\mathbf{k}j}^l)^* \quad (7)$$

where  $R_{\mathbf{k}j}$  is a complex-valued Gaussian noise integrated over  $\Delta t$  to give a variance  $\langle R_{\mathbf{k}'j'}^l R_{\mathbf{k}j}^l \rangle = V^{-1} N_\tau^{-1} \delta_{\mathbf{k},-\mathbf{k}'} \delta_{j,-j'} \delta_{l,l'} [(1 - \exp(-2A_{\mathbf{k}j}\Delta t)/2A_{\mathbf{k}j})]$ , and superscripts indicate time-step indices,  $l = t/\Delta t$ . With the use of fast Fourier transform (FFT) methods, this algorithm has a computational cost that scales approximately linearly with both system volume and  $N_\tau$ , while the cost per CL time step is independent of the number of bosons.

*Results:* We begin by demonstrating that our sampling scheme can reproduce the thermodynamics of an ideal Bose gas with  $U_{\text{ext}}(\mathbf{r}) = 0$ ,  $v(\mathbf{r}) = 0$ . Fig. 1 shows the logarithm of the activity,  $\ln(z) = \beta\mu$ , versus a dimensionless particle density that is independent of boson mass. We compare to a reference result[29]  $\frac{N\Lambda^3}{V} = \text{Li}_{3/2}(z)$ , where  $\Lambda = h(2\pi mk_B T)^{-1/2}$  is the de Broglie thermal wavelength, and Li is the polylogarithm function, which is a good closed-form approximation to the exact density if the ground-state population vanishes (i.e., outside BEC).

For low densities, an ideal Bose gas behaves thermodynamically as a classical assembly of distinguishable particles obeying Boltzmann statistics. As the phase-space density increases, quantum effects become increasingly important. At  $N\Lambda^3/V \sim 1$ , the average interparticle spacing is on the order of the de Broglie thermal wavelength, indicating an approximate crossover to quantum degeneracy and an increased importance of particle-exchange statistics. All particle exchanges along the imaginary time paths are properly counted by the coherent-states field theory, without any special sampling requirements. The crossover to BEC (not shown in Fig. 1) can be approximated by  $\text{Li}_{3/2}(1) \approx 2.61$ , corresponding to the chemical potential  $\mu \rightarrow 0^-$ ; beyond this limit the polylogarithm approximation to the phase-space density breaks down, because that result was derived assum-

(ETD) algorithm[27, 28]. Values of non-linear components are taken from the previous time step over the whole  $\Delta t$  interval resulting in a method that is weak first-order accurate with excellent stability. Linear contributions to the equation of motion are integrated exactly over the interval, hence purely linear problems (i.e., those for which  $v = 0$ ) are in principle accurately propagated to all orders in  $\Delta t$ . The resulting algorithm is

ing zero population of the ground state. We note that in this example, CL simulations are also restricted to  $\mu < 0$  because there is no repulsion to stabilize against divergent particle numbers obtained once  $\mu > \epsilon_0$ , where  $\epsilon_0$  is the ground-state energy of the one-body Hamiltonian (i.e., the action is unbounded, and the BEC phase is not directly accessible to the simulation when  $v = 0$ ).

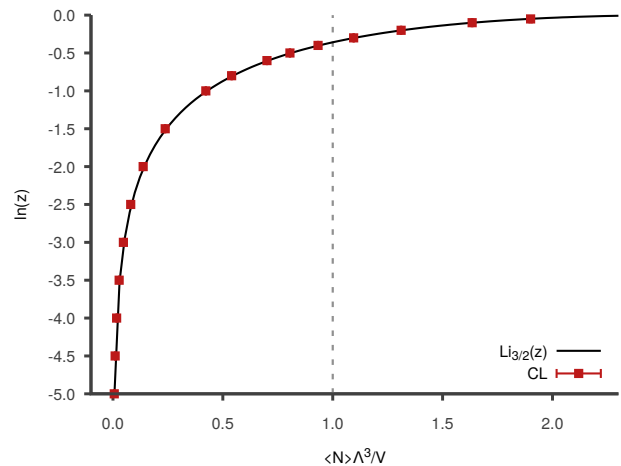


FIG. 1. (Color online): Equation of state for a Bose ideal gas computing using the coherent-states complex-Langevin sampling method (red points).  $\ln(z) = \beta\mu$  is the logarithm of the activity, and the phase-space density is made dimensionless using the thermal wavelength  $\Lambda$ . The reference result is the  $3/2$  polylogarithm (see body text). Error bars are stochastic errors of the mean.

A  $\phi^4$  scalar field theory results from a pair interaction potential  $v(r) = v_0 \delta(r)$ . The parameter  $v_0$  can be chosen as a pseudopotential to mimic a realistic inter-atomic potential in a low-energy approximation by preserving the s-wave scattering length,  $a_s$ , as  $v_0 = 4\pi\hbar^2 a_s m^{-1}$ . In the

present case, we treat  $v_0$  as an arbitrary model parameter and compare CL simulation predictions for the  $\lambda$  line of critical phase transitions to analytic theory. The reference critical temperature for this model, obtained from a renormalization group analysis and mapping the critical behavior onto a classical spin model[30–32], is

$$k_B T_c = \frac{2\pi\hbar^2}{m} \left( \frac{\mu}{2v_0\zeta(3/2)} \right)^{2/3}, \quad (8)$$

where  $\zeta$  is the Riemann zeta function.

For our simulations of the  $\phi^4$  theory, we write the action with a minimal set of parameters by choosing a nondimensionalization strategy that scales lengths by the thermal wavelength,  $\Lambda_{\text{ref}}$ , at a reference temperature,  $T_{\text{ref}}$ , so that  $T^* = T/T_{\text{ref}}$  and  $\mu^* = \mu/k_B T_{\text{ref}}$  remain explicit in the action. We locate the critical temperature using the Bose condensate fraction,  $\langle \tilde{N}_0 \rangle / \langle \tilde{N} \rangle$ , as an order parameter, where  $\tilde{N}_0 = V N_\tau^{-1} \sum_{n=0}^{N_\tau-1} \hat{\varphi}_{n,\mathbf{k}=0}^* \hat{\varphi}_{n-1,\mathbf{k}=0}$  and  $\hat{\varphi}$ ,  $\hat{\varphi}^*$  are the spatial Fourier transforms of  $\varphi$ ,  $\varphi^*$ . Although the order parameter in the thermodynamic limit is non-zero only for  $T < T_c$ , in common with other critical phase transitions, finite-size errors dramatically modify the value in the region of  $T_c$  making the phase transition difficult to extract, as shown in Fig. 2(a). We apply a finite-size scaling analysis[33], shown in Fig. 2(b), to extract  $T_c$ . This approach is explained in detail in the Supplementary Material[34], and two other forms of scaling analysis are there shown to be consistent. Finally, Fig. 3 shows the full  $\mu$ -dependent CL phase diagram for  $v_0^* = v_0/(k_B T_{\text{ref}} \Lambda_{\text{ref}}^3) = 0.005$  and 0.010 compared to Eqn. 8.

A thorough analysis of factors affecting computational cost is beyond the scope of the present work, but we report here the approximate timing for a single simulation on a single hardware platform for illustration. A large-cell simulation sampled with a  $32 \times 32 \times 32$  spatial collocation mesh and  $N_\tau = 100$  takes 10–15 ms per CL time step on an NVIDIA Tesla V100 GPU[35]. We have found  $2.5 \times 10^6$  time steps to yield an error of the mean of the condensate fraction below 0.1%, requiring 7–11 hours on the V100 GPU.

*Canonical Ensemble:* The field theory presented here is formulated at fixed chemical potential, and direct control of particle number is not immediately possible. However, there are often situations where constraining particle number is convenient or required, e.g., in limiting simulations of bosons in an optical lattice to integer fill fractions[11]. In order to perform simulations in the canonical ensemble, we write the canonical partition function as

$$Z(N, V, T) = \int \mathcal{D}(\varphi, \varphi^*) \delta(N - \tilde{N}[\varphi, \varphi^*]) e^{-S_0}, \quad (9)$$

where  $S_0$  is equal to the action of Eqn. 2 with  $\mu = 0$ , and  $\tilde{N}[\varphi, \varphi^*]$  is the particle-number operator introduced

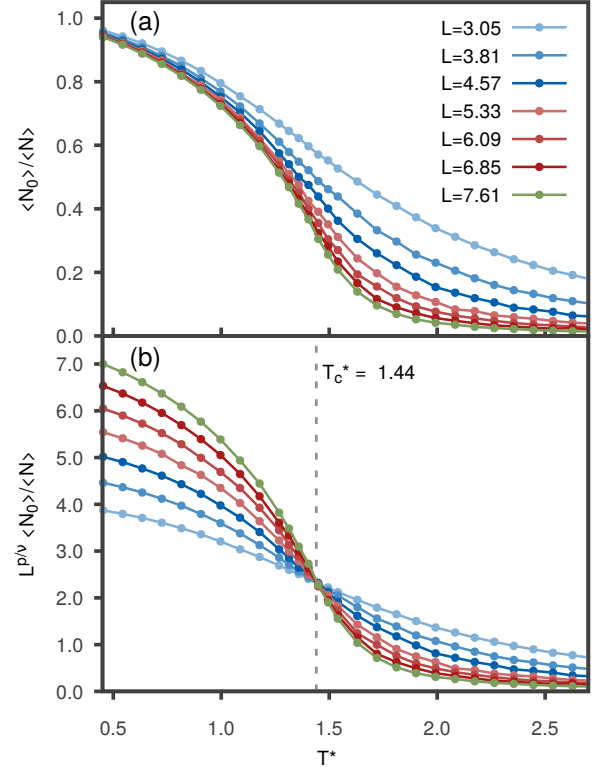


FIG. 2. (Color online): (a) the Bose condensate fraction for various simulation cell sizes ( $L = 3.05$ – $7.61$  in multiples of  $\Lambda_{\text{ref}}$ ),  $\mu^* = 0.045$ , and  $v_0^* = 0.005$ , shows large finite-size errors. Errors of the mean are smaller than the symbol size. Numerical discretization parameters are  $\Delta t = 0.05$ ,  $N_\tau = 50$ , and spatial collocation mesh spacing  $\Delta x = 0.28 \Lambda_{\text{ref}}$ . (b) Finite-size scaling analysis of the condensate fraction allows  $T_c^*$  to be extracted. In this work,  $\nu = 0.671$  and  $p = 0.45$  (see Supplementary Material[34]).

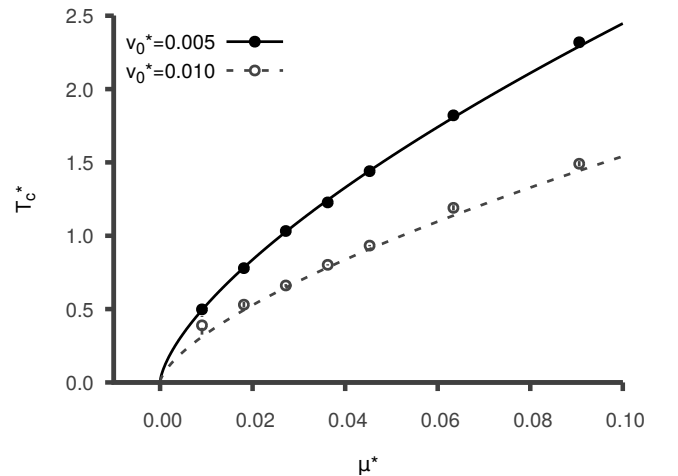


FIG. 3. Critical temperature versus chemical potential,  $T_c^*(\mu^*)$ , for the  $\phi^4$  theory. Points are from complex Langevin (CL) simulations and finite-size scaling analysis (see Supplementary Material[34]); lines are from Eqn. 8.

previously. By writing the Dirac delta function in exponential notation, a new scalar integration variable is introduced:

$$Z(N, V, T) = \frac{1}{2\pi} \int_{-\infty}^{\infty} dw \int \mathcal{D}(\varphi, \varphi^*) e^{-S_0 - iw(N - \tilde{N}[\varphi, \varphi^*])}. \quad (10)$$

By identifying  $iw = \beta\mu$ , the new ensemble can be sampled using the same CL equations as those for the grand-canonical ensemble, but with a complex-valued, time-dependent chemical potential sampled according to the following equation of motion:

$$\partial_t \mu(t) = \lambda_\mu \beta^{-1} \left( N - \tilde{N}[\varphi, \varphi^*] \right) + i\eta_\mu(t), \quad (11)$$

where  $\eta_\mu$  is a real-valued Gaussian-distributed random variable with variance  $\langle \eta_\mu(t) \eta_\mu(t') \rangle = 2\lambda_\mu \delta(t - t')$  and  $\lambda_\mu$  is a mobility coefficient that controls the rate of evolution of  $\mu$  relative to the coherent-states fields. We time step this equation—in tandem with the field CL equations—using an explicit Euler-Maruyama algorithm. A numerical demonstration of the particle-number-constraint method for the ideal Bose gas is shown in the Supplementary Material[34]. The strategy described here constitutes a general way of adding constraints in sampling the field theory.

*Conclusions:* We have presented a new algorithm for directly simulating the coherent-states path integral field theory of interacting bosons using complex Langevin dynamics and pseudospectral collocation with exponential time differencing. We have demonstrated the method by extracting the  $\lambda$  line of critical phase transitions of a  $\phi^4$  scalar field theory. Although the field theory is formulated and directly applied in the grand-canonical ensemble, we have shown a route to simulations in the canonical ensemble for the cases that require precise control of the particle number.

The method presented here is broadly applicable to bosonic quantum field theories. It immediately generalizes to continuous space models with arbitrary pair interactions and external confining potentials (e.g., optical lattices[11]). Discrete lattice models, such as the Bose-Hubbard model, require only minor modifications to the linear coefficients  $A_{\mathbf{k}j}$  of Eqns. 4–5 to reflect the discrete kinetic-energy (hopping) operator. Similarly, a vast array of quantum-spin lattice models (ferromagnetic, antiferromagnetic, w/o frustration) in second-quantized form using the Schwinger boson representation[36] should be accessible to the present algorithm. Although convergence of the complex Langevin trajectories is not guaranteed and is yet to be tested on this diverse set of models, in the cases that convergence is achieved the exponential of the action is guaranteed to be correctly sampled and equilibrium properties can be computed without bias. Finally, by transforming the current imaginary time dependence to a closed real-time Keldysh contour[37], a broad range of finite temperature, quantum dynamical

phenomena could be explored. This includes both real-time Green functions for linear response properties and far-from-equilibrium dynamics.

We thank Matthew Fisher and David Weld for helpful discussions. KTD and GHF were partially supported by the National Science Foundation grant DMR-1822215. Simulations were performed using the computational facilities purchased with funds from the National Science Foundation (CNS-1725797) and administered by the Center for Scientific Computing (CSC). The CSC is supported by the California NanoSystems Institute and the Materials Research Science and Engineering Center (MRSEC; NSF DMR 1720256) at UC Santa Barbara.

- 
- [1] P. Kapitza, *Nature* **141**, 74 (1938).
  - [2] J. F. Allen and A. D. Misener, *Nature* **141**, 75 (1938).
  - [3] F. London, *Nature* **141**, 643 (1938).
  - [4] R. P. Feynman, *Statistical Mechanics (Frontiers in Physics)* (W.A. Benjamin, 1972).
  - [5] K. B. Davis, M. O. Mewes, M. R. Andrews, N. J. van Druten, D. S. Durfee, D. M. Kurn, and W. Ketterle, *Phys. Rev. Lett.* **75**, 3969 (1995).
  - [6] E. L. Raab, M. Prentiss, A. Cable, S. Chu, and D. E. Pritchard, *Phys. Rev. Lett.* **59**, 2631 (1987).
  - [7] W. Ketterle and N. V. Druten, in *Advances In Atomic, Molecular, and Optical Physics* (Elsevier, 1996) pp. 181–236.
  - [8] M. P. A. Fisher, P. B. Weichman, G. Grinstein, and D. S. Fisher, *Phys. Rev. B* **40**, 546 (1989).
  - [9] D. Jaksch, C. Bruder, J. I. Cirac, C. W. Gardiner, and P. Zoller, *Phys. Rev. Lett.* **81**, 3108 (1998).
  - [10] M. Greiner, O. Mandel, T. Esslinger, T. W. Hänsch, and I. Bloch, *Nature* **415**, 39 (2002).
  - [11] S. Trotzky, L. Pollet, F. Gerbier, U. Schnorrberger, I. Bloch, N. V. Prokof'ev, B. Svistunov, and M. Troyer, *Nat. Phys.* **6**, 998 (2010).
  - [12] D. M. Ceperley, *Rev. Mod. Phys.* **67**, 279 (1995).
  - [13] E. L. Pollock and K. J. Runge, *Phys. Rev. B* **46**, 3535 (1992).
  - [14] W. Krauth, *Phys. Rev. Lett.* **77**, 3695 (1996).
  - [15] P. Grüter, D. Ceperley, and F. Laloë, *Phys. Rev. Lett.* **79**, 3549 (1997).
  - [16] D. M. Ceperley and B. Bernu, *Phys. Rev. Lett.* **93**, 155303 (2004).
  - [17] B. K. Clark and D. M. Ceperley, *Phys. Rev. Lett.* **96**, 105302 (2006).
  - [18] M. Boninsegni, N. Prokof'ev, and B. Svistunov, *Phys. Rev. Lett.* **96**, 070601 (2006).
  - [19] J. W. Negele and H. Orland, *Quantum Many-particle Systems (Advanced Books Classics)* (Perseus Books, 1998).
  - [20] G. Parisi, *Phys. Lett. B* **131**, 393 (1983).
  - [21] J. R. Klauder, *J. Phys. A* **16**, L317 (1983).
  - [22] S. Lee, *Nucl. Phys. B* **413**, 827 (1994).
  - [23] G. Aarts and I.-O. Stamatescu, *J. High Energy Phys.* **09** (2008), 018.
  - [24] G. Aarts, *Phys. Rev. Lett.* **102**, 131601 (2009).
  - [25] F. Attanasio and B. Jäger, *Eur. Phys. J. C* **79**, 16 (2019).
  - [26] X. Man, K. T. Delaney, M. C. Villet, H. Orland, and

- G. H. Fredrickson, J. Chem. Phys. **140**, 024905 (2014).
- [27] M. C. Villet and G. H. Fredrickson, J. Chem. Phys. **132**, 034109 (2010).
- [28] D. Düchs, K. T. Delaney, and G. H. Fredrickson, J. Chem. Phys. **141**, 174103 (2014).
- [29] L. D. Landau and E. M. Lifshitz, *Statistical Physics, Part 1 (Course of Theoretical Physics, Vol. 5)*, 3rd ed. (Pergamon Press, 1980).
- [30] M. Rasolt, M. J. Stephen, M. E. Fisher, and P. B. Weichman, Phys. Rev. Lett. **53**, 798 (1984).
- [31] P. B. Weichman, M. Rasolt, M. E. Fisher, and M. J. Stephen, Phys. Rev. B **33**, 4632 (1986).
- [32] S. Sachdev, *Quantum Phase Transitions* (Cambridge University Press, 2011).
- [33] Michael N. Barber, “Finite-size Scaling,” in *Phase Transitions and Critical Phenomena*, Vol. 8, edited by C. Domb and J. L. Lebowitz (Academic Press, 1983) Chap. 2.
- [34] See Supplementary Material [url] for the finite-size scaling analyses of  $T_c$  and a numerical demonstration of applying the particle-number constraint method. The Supplementary Material includes Refs. [38, 39].
- [35] K. T. Delaney and G. H. Fredrickson, Comput. Phys. Commun. **184**, 2102 (2013).
- [36] D. P. Arovas and A. Auerbach, Phys. Rev. B **38**, 316 (1988).
- [37] A. Kamenev, *Field Theory of Non-Equilibrium Systems* (Cambridge University Press, 2011).
- [38] R. Guida and J. Zinn-Justin, “Critical exponents of the N-vector model,” Journal of Physics A: Mathematical and General **31**, 8103–8121 (1998).
- [39] K. Binder, “Critical Properties from Monte Carlo Coarse Graining and Renormalization,” Phys. Rev. Lett. **47**, 693–696 (1981).